Journal of Sound and Vibration 329 (2010) 261–276

Contents lists available at ScienceDirect

Journal of Sound and Vibration

journal homepage: www.elsevier.com/locate/jsvi

Vibration confinement and energy harvesting in flexible structures using collocated absorbers and piezoelectric devices

M. Ouled Chtiba [a], S. Choura [a,*], A.H. Nayfeh [b], S. El-Borgi [a]

[a] Applied Mechanics Research Laboratory, Tunisia Polytechnic School, La-Marsa, Tunisia
[b] Department of Engineering Sciences and Mechanics, Virginia Tech, Blacksburg, VA, USA

ARTICLE INFO

Article history:
Received 23 March 2009
Received in revised form
21 September 2009
Accepted 22 September 2009
Handling Editor: A.V. Metrikine

ABSTRACT

We propose an optimal design for supplementing flexible structures with a set of absorbers and piezoelectric devices for vibration confinement and energy harvesting. We assume that the original structure is sensitive to vibrations and that the absorbers are the elements where the vibration energy is confined and then harvested by means of piezoelectric devices. The design of the additional mechanical and electrical components is formulated as a dynamic optimization problem in which the objective function is the total energy of the uncontrolled structure. The locations, masses, stiffnesses, and damping coefficients of these absorbers and capacitances, load resistances, and electromechanical coupling coefficients are optimized to minimize the total energy of the structure. We use the Galerkin procedure to discretize the equations of motion that describe the coupled dynamics of the flexible structure and the added absorbers and harvesting devices. We develop a numerical code that determines the unknown parameters of a pre-specified set of absorbers and harvesting components. We input a set of initial values for these parameters, and the code updates them while minimizing the total energy in the uncontrolled structure. To illustrate the proposed design, we consider a simply supported beam with harmonic external excitations. Here, we consider two possible configurations for each of the additional piezoelectric devices, either embedded between the structure and the absorbers or between the ground and absorbers. We present simulations of the harvested power and associated voltage for each pair of collocated absorber and piezoelectric device. The simulated responses of the beam show that its energy is confined and harvested simultaneously.

1. Introduction

Recent years have seen the emergence of many developments in the field of so-called smart structures; that is, structures incorporating sensors and actuators coupled with a calculator and are able to control dynamic systems subject to external excitations. Among the many types of materials that can be found in nature, piezoelectric materials have a good ability of electromechanical conversion and small sizes, which simplify their use in widely dynamic structure applications. Recently, the piezoelectric material is used to harvest energy from excited structures. Energy harvesting or energy scavenging is the process by which energy is captured and stored. A variety of different sources exist for harvesting energy, such as solar power, thermal energy, wind, and kinetic energy.

* Corresponding author.
E-mail address: s_choura@yahoo.com (S. Choura).

0022-460X/$ - see front matter © 2009 Elsevier Ltd. All rights reserved.
doi:10.1016/j.jsv.2009.09.028

The use of piezoelectric materials to harvest power has already become popular. In the literature, a significant number of studies developed accurate models and discussed in great details the fundamentals of these materials and their usage to harvest energy. These studies include the works of Sodano et al. [1], Feenstra et al. [2], Shahruz [3], Stephen [4], Ng and Liao [5], Cornwell et al. [6], Yoon et al. [7], Lefeuvre et al. [8], Liu et al. [9], Beeby et al. [10], Swallow et al. [11], Sari et al. [12], Sodano et al. [13,14], Williams and Yates [15], Mateu and Moll [16], Sodano et al. [17], and Lesieutre et al. [18]. Sodano and Inman [19] provided a review of modern techniques for power harvesting of vibrations using piezoelectric materials and discussed their everyday applications. They concluded that the use of piezoelectric materials is the major method of harvesting energy. Sodano et al. [1] developed a model of the piezoelectric material power harvesting device. This model simplifies the design procedure for determining the appropriate size and vibration levels necessary for sufficient energy to be produced and supplied to the electronic devices. An experimental verification of the model was also performed to ensure its accuracy. Sodano et al. [17] investigated three types of piezoelectric devices and experimentally tested them to determine their abilities to transform ambient vibration into electrical energy and their capabilities to recharge a discharged battery. Stephan [4] analyzed the extraction of energy from a vibrating environment in some details. He deduced that, for both direct mass (force) and base excitation, the maximum power flow into the device depends on the vigor of the environment (frequency and amplitude of force or base) and the size of the device.

Stephan [4] and Jeon et al. [20] modeled the damping coefficient to be the sum of mechanical and electrical terms. Stephan [4] noted that maximum power is delivered to an electrical load when its resistance is equal to the sum of the coil internal resistance and the electrical analog of the mechanical damping coefficient. Sodano et al. [13] claimed that the process of generation and dissipation of eddy current causes the system to function as a viscous damper. They developed a model for one eddy current damping system and showed that it is effective in the suppression of transverse beam vibrations. Lesieutre et al. [21] investigated the damping added to a structure due to the removal of electrical energy from the system during power harvesting. They first estimated the damping using analytical methods and later verified it experimentally.

Wu and Wang [22] investigated the feasibility of utilizing eigenvector assignment and piezoelectric circuitry for enhancing vibration isolation performance of periodic isolators. They used this strategy to reduce the transmissibility of the isolator modes near the boundary of the stop bands, thereby widening the effective frequency range of vibration suppression of the periodic isolator. The integrated system with assigned eigenvectors redistributes the vibratory energy of the complete electromechanical system. Small vibration at the attenuated end of the isolator is achieved because the energy is confined in the circuitry and other parts of the isolator. Yoon [23] proposed a full-state feedback control strategy to confine the vibratory motion of flexible structures. He used small segments of piezoelectric film as sensors. The proposed approach was demonstrated by an experiment in which two piezoelectric patch actuators confine the vibration of a pinned–pinned beam using two piezoelectric polyvinylidene fluoride (PVDF) patches as sensors.

Yigit and Choura [24] and Choura and Yigit [25,26] developed a strategy for active control of vibrations by confinement. Their strategy consists of assigning the eigenstructure (both eigenvalues and eigenvectors) of flexible structures for the purpose of simultaneous confinement and suppression of vibrations where the modal matrix plays a key role in the energy redistribution. Such strategy guarantees both vibration confinement and structural stability. Ouled Chtiba et al. [27] discussed hybrid control of seismically excited structures by vibration confinement. Their control strategy consists of adding bracing elements as the nonsensitive elements of the modified structure. Then active controllers were used to remove the vibration energy from the floors and transfer it to the bracing elements. Ouled Chtiba et al. [28] developed a strategy of vibration confinement that transforms an LQR-based active controller to an equivalent passive controller. They demonstrated that both control strategies lead to similar structural performance.

Following Ouled Chtiba et al. [29], the current study is concerned with the confinement and harvesting of vibrations in flexible structures by adding a set of collocated absorbers and piezoelectric elements. The proposed design aims at transferring the vibration energy from the flexible structure to the absorbers and confining it into these elements. We collocate at each absorber a piezoelectric device to store the cultivated electrical power into batteries. The problem of confining and harvesting vibrations is formulated as a dynamic optimization problem whose solution provides a set of absorber parameters (masses, locations, stiffnesses, and damping coefficients) and piezoelectric elements (electromechanical coupling coefficients, capacitances and loaded resistances). The objective function, associated with the optimization problem, minimizes the total energy (strain and kinetic) of the uncontrolled structure. With the aid of the Matlab optimization toolbox, we develop a computer code that outputs a set of optimized mechanical and electrical parameters. In particular, we use the *fmincon* command, which uses the sequential quadratic programming as an optimal integrator, and the *ode*15*s* command, as a linear solver of the ordinary-differential equations that govern the dynamics of the modified structure.

2. Electromechanical model

We develop a mathematical model of the electromechanical system formed of a set of mass-damper-spring absorbers and piezoelectric devices. Several mechanical architectures of vibration-based power generators are possible. In the case of piezoelectric generators, energy conversion is maximized by a maximum deformation of the piezoelectric material. This explains why most of the reported devices are optimized for working at a resonance frequency [4]. Near a resonance frequency, a single degree-of-freedom absorber gives a good description of a vibrating structure. And in most cases, the problem can be simplified by considering only one vibration mode. If the mechanical structure is vibrating with little

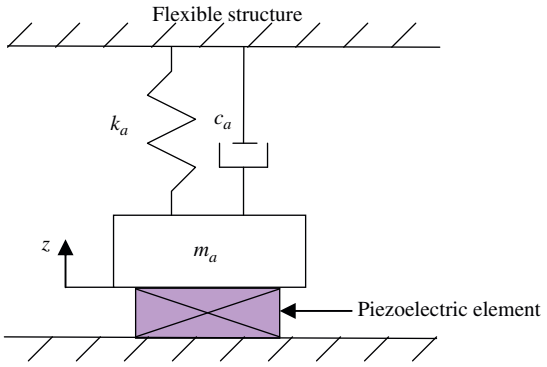

Fig. 1. Model of an absorber including a piezoelectric element.

displacements for which the motion remains linear, then the structure including the piezoelectric element can be simply modeled by the mass-damper-spring-piezo device shown in Fig. 1.

Following Lefeuvre et al. [8], we consider the piezoelectric element to be a disk with a rigid mass m bonded on its top side. The bottom side of the disk is bonded on a reference rigid base. In addition, the stiffness and losses of the mechanical part are, respectively, modeled by a spring k_a and viscous damper c_a. The rigid mass m_a is subject to the action of both external and internal forces. The external force F_a results from the mechanical excitation applied to the structure. The internal force can be separated into a restoring force F_P due to the piezoelectric element, a restoring force due to the spring, and a viscous force due to the damper.

We let z be the mass displacement and Q_p and V be, respectively, the output electrical charge and voltage across the electrodes of the piezoelectric element. For a piezoelectric disk, the constitutive equations relating the stress T_p and electrical induction D_p to the strain S_p and electric field E_p, are

$$T_p = c_{33}^E S_p - e_{33} E_p \tag{1a}$$

$$D_p = e_{33} S_p + \varepsilon_{33}^S E_p \tag{1b}$$

where c_{33}^E is the elastic rigidity in short circuit configurations, e_{33} is the piezoelectric coefficient, and ε_{33}^S is the clamped permittivity. The equations relating the mechanical variables (z and F_P) to the electrical variables (Q_p and V) are

$$F_p = K_{PE} z + \theta V \tag{2a}$$

$$Q_p = \theta z - C_p V \tag{2b}$$

where E_p, S_p, Q_p, F_p, K_{PE}, C_p, and θ are defined by

$$E_p = -\frac{V}{e_p}, S_p = \frac{z}{e_p}, Q_p = A_p D_p, F_p = A_p T_p \tag{3a}$$

$$K_{PE} = \frac{c_{33}^E A_p}{e_p}, C_p = \frac{\varepsilon_{33}^S A_p}{e_p}, \theta = \frac{e_{33} A_p}{e_p} \tag{3b}$$

Here, K_{PE} is the stiffness of the piezoelectric element when it is short-circuited, C_p is the clamped capacitance, θ is its electromechanical coupling coefficient, and e_p is the thickness. The equivalent stiffness for both of the mechanical absorber and the piezoelectric element is given by

$$k = K_{PE} + k_a \tag{4}$$

Substituting the piezoelectric force (Eq. (2a)) and mechanical forces of the absorber and noting that $V = C_p^{-1} Q_p$ yields the absorber dynamical equation

$$m_a \ddot{z} + c_a \dot{z} + k_a z + F_p = m_a \ddot{z} + c_a \dot{z} + kz + \theta C_p^{-1} Q_p = F_a \tag{5}$$

The voltage output of the system across the load resistance R is defined by $V = R\dot{Q}_p$. Eq. (2b) simplifies to

$$R\dot{Q}_p - C_p^{-1}\theta z + C_p^{-1} Q_p = 0 \tag{6}$$

Solutions of Eqs. (5) and (6) yield the electric response of the absorber-piezo system.

3. Dynamic optimization

We consider an electromechanical system composed of a flexible structure and a set of collocated absorbers and piezoelectric devices. This coupled dynamics is described by the following discretized model:

$$\begin{bmatrix} M_s & 0 \\ 0 & M_a \end{bmatrix} \begin{bmatrix} \ddot{X}_s \\ \ddot{X}_a \end{bmatrix} + \begin{bmatrix} C_s & C_{sa} \\ C_{sa}^T & C_a \end{bmatrix} \begin{bmatrix} \dot{X}_s \\ \dot{X}_a \end{bmatrix} + \begin{bmatrix} K_s & K_{sa} \\ K_{sa}^T & K_a \end{bmatrix} \begin{bmatrix} X_s \\ X_a \end{bmatrix} - \begin{bmatrix} 0 \\ \Theta C_p^{-1} \end{bmatrix} Q = \begin{bmatrix} F_s \\ F_a \end{bmatrix} \tag{7a}$$

$$R\dot{Q} - C_p^{-1}\Theta^T(X_a - \Phi X_s) + C_p^{-1}Q = 0 \tag{7b}$$

where M_s, C_s, and K_s are the $m \times m$ mass, damping, and stiffness matrices of the unaltered flexible structure, respectively; X_s is the $m \times 1$ structural displacement vector; M_a, C_a, and K_a are the $n \times n$ mass, damping, and stiffness matrices of the added absorbers, respectively; C_{sa} and K_{sa} are the $m \times n$ damping and stiffness coupling matrices, respectively; X_a is the $n \times 1$ absorber displacement vector; F_s and F_a are the external loading vectors associated with the structure and absorbers, respectively; Θ is the $n \times n$ electromechanical coupling matrix; C_p is the $n \times n$ capacitance matrix; R is the $n \times n$ loaded resistance matrix; Q is the $n \times 1$ charge vector; and Φ is a $n \times m$ transformation matrix. The matrix Φ is zero in case the piezoelectric elements are placed between the absorber masses and ground and nonzero if they are placed between the absorber masses and the flexible structure.

System (7) can be put in the following first-order form

$$\begin{bmatrix} \dot{X}_s \\ \dot{X}_a \\ \ddot{X}_s \\ \ddot{X}_a \\ \dot{Q} \end{bmatrix} = \begin{bmatrix} 0 & 0 & I_{m\times m} & 0 & 0 \\ 0 & 0 & 0 & I_{n\times n} & 0 \\ -M_s^{-1}K_s & -M_s^{-1}K_{sa} & -M_s^{-1}C_s & -M_s^{-1}C_{sa} & 0 \\ -M_a^{-1}K_{sa}^T & -M_a^{-1}K_a & -M_a^{-1}C_{sa}^T & -M_a^{-1}C_a & M_a^{-1}\Theta C_p^{-1} \\ -R^{-1}C_p^{-1}\Theta^T\Phi & R^{-1}C_p^{-1}\Theta^T & 0 & 0 & -R^{-1}C_p^{-1} \end{bmatrix} \begin{bmatrix} X_s \\ X_a \\ \dot{X}_s \\ \dot{X}_a \\ Q \end{bmatrix} + \begin{bmatrix} 0 \\ 0 \\ M_s^{-1}F_s \\ M_a^{-1}F_a \\ 0 \end{bmatrix} \tag{8}$$

where the vector $\dot{Q}$ represents the current outputs of the piezoelectric elements.

Dynamic modeling of most engineering processes results in a set of differential equations. The dynamic optimization of these processes examines their performance under transient conditions and optimizes it by maximizing or minimizing a performance index subject to operating constraints. Applications of dynamic optimization include determination of the controller parameters, which is essential for the design and control of structural engineering systems. The solution is carried out in the full space of variables. However, this method results in a nonlinear problem with a large number of variables and nonlinear equality and inequality constraints.

In the last decades, several studies used dynamic optimization to develop robust controllers. Tanartkit and Biegler [30] presented a simultaneous approach for dynamic optimization by discretizing the variables through collocation on finite elements. They considered solution of the nonlinear programming problem through a reduced Hessian successive quadratic programming approach. Cervantes and Biegler [31] solved the dynamic optimization problem using a reduced-space successive quadratic programming algorithm. The system is stabilized without imposing new boundary conditions. Richard et al. [32] used dynamic optimization to adapt a 3-DOF robot to a pre-defined trajectory, which has mechanical constraints. Santos and Biegler [33] developed a strategy, based on nonlinear programming sensitivity, to establish stability bounds on the plant/model mismatch for a class of optimization-based model predictive control algorithms. They derived a sufficient condition for robust stability of the controllers. Ouled Chtiba et al. [29] designed a set of dynamic absorbers to confine the vibrational energy of the unaltered structure. These absorbers are formulated as a dynamic optimization problem in which the objective function is the total energy of the uncontrolled structure.

In the current study, we formulate and then solve a dynamic optimization problem that outputs a set of mechanical and electrical parameters of the added absorbers and piezoelectric elements. In particular, we minimize the total energy (kinetic and strain energies) of the unaltered structure, which is considered to be sensitive to vibration, to confine and harvest the vibration energy in the added absorbers. Without loss of generality, the problem is formulated as follows:

$$\min_{p_a} J = \frac{1}{2}\int_0^{t_f} (\dot{X}_s^T M_s \dot{X}_s + X_s^T K_s X_s)\,\mathrm{d}t$$

subject to

$$\begin{bmatrix} \dot{X}_s \\ \dot{X}_a \\ \ddot{X}_s \\ \ddot{X}_a \\ \dot{Q} \end{bmatrix} = \begin{bmatrix} 0 & 0 & I_{m\times m} & 0 & 0 \\ 0 & 0 & 0 & I_{n\times n} & 0 \\ -M_s^{-1}K_s & -M_s^{-1}K_{sa} & -M_s^{-1}C_s & -M_s^{-1}C_{sa} & 0 \\ -M_a^{-1}K_{sa}^T & -M_a^{-1}K_a & -M_a^{-1}C_{sa}^T & -M_a^{-1}C_a & M_a^{-1}\Theta C_p^{-1} \\ -R^{-1}C_p^{-1}\Theta^T\Phi & R^{-1}C_p^{-1}\Theta^T & 0 & 0 & -R^{-1}C_p^{-1} \end{bmatrix} \begin{bmatrix} X_s \\ X_a \\ \dot{X}_s \\ \dot{X}_a \\ Q \end{bmatrix}, \forall t \in [0, t_f] \tag{9}$$

$$g(p_a) \leq 0$$
$$h(p_a) = 0$$
$$p_a^L \leq p_a \leq p_a^U$$
$$X_s(0, p_a) = X_0(p_a)$$
$$X_a(0, p_a) = Z_0(p_a)$$
$$Q(0, p_a) = Q_0(p_a)$$

where J is the objective function, g is the constraint inequality, h is the constraint equality, X_0 is the initial displacement vector of the unaltered structure, Z_0 is the initial absorber displacement vector, Q_0 is the initial charge vector, t is time, and t_f is the final time. Here, we aim at determining a set of optimized parameters p_a by minimizing the total energy of the dynamical system subject to the dynamical differential equations without inequality. Here, p_a^L and p_a^U are the lower and upper bound vectors of the absorber and piezoelectric parameters. The resulting optimized absorbers and piezoelectric elements must guarantee vibration confinement in the added absorbers and harvesting the confined energy.

To demonstrate the viability of the proposed dynamic optimization approach, we consider the vibration confinement and harvesting of a simply supported beam of flexural rigidityEI, mass par unit length ρA, and length L. We equip the beam with a set of n sets of collocated absorbers and piezoelectric elements, as shown in Fig. 2. The masses, spring stiffnesses, damping coefficients, and locations are designated by m_i, k_i, c_i, and x_i ($i = 1, 2, \ldots, n$). The variables $w(x, t)$ and z_i denote, respectively, the transverse vibration of the beam and the displacement of the ith absorber. Here, we consider two cases of piezoelectric element configurations: embedding the piezoelectric elements between the beam and absorber masses (Fig. 3) and between the ground and the absorber masses (Fig. 4).

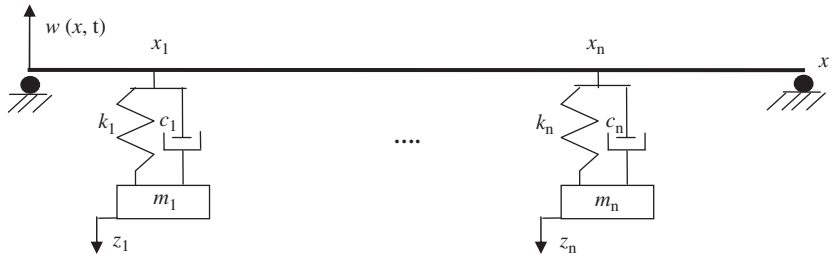

Fig. 2. Beam equipped with absorbers.

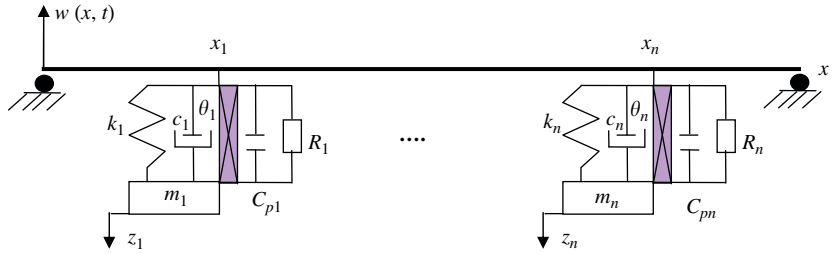

Fig. 3. Configuration 1: piezoelectric elements between the absorber masses and the beam.

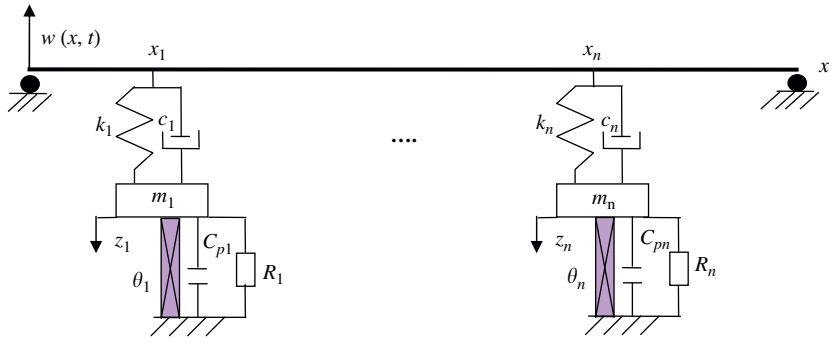

Fig. 4. Configuration 2: piezoelectric elements between the absorber masses and the ground.

4. Configuration 1

In this case, the piezoelectric elements are embedded between the beam and the absorber masses. The equations of motion that describe the coupled dynamics of the beam-absorber-piezoelectric system of Fig. 3 are given by

$$EI\frac{\partial^4 w(x,t)}{\partial x^4}+\rho A\frac{\partial^2 w(x,t)}{\partial t^2}=-\sum_{i=1}^{n}\left[k_i(w(x_i,t)-z_i)+c_i\left(\frac{\partial w(x_i,t)}{\partial t}-\dot{z}_i\right)\right]\delta(x-x_i) \tag{10a}$$

$$m_i\ddot{z}_i+c_i\dot{z}_i+k_iz_i-\frac{\theta_i}{C_{pi}}Q_i=k_iw(x_i,t)+c_i\frac{\partial w(x_i,t)}{\partial t}\quad \text{for } i=1,2,\ldots,n \tag{10b}$$

$$R_i\dot{Q}_i-\frac{\theta_i}{C_{pi}}(z_i-w(x_i,t))+\frac{Q_i}{C_{pi}}=0\quad \text{for } i=1,2,\ldots,n \tag{10c}$$

where $\delta(x)$ is the Dirac delta function, θ_i is the electromechanical coupling coefficient, R_i is the loaded resistance, and C_{pi} is the capacitance of the ith piezoelectric element. The set of mechanical and electrical parameters ($m_i, c_i, k_i, x_i, R_i, C_{pi}$, and$\theta_i$) are determined using dynamic optimization.

The key idea of the proposed design is to transfer the total energy of the unaltered structure to the added elements and then harvest it. The total energy of the beam is given by

$$E_b(t)=T_b(t)+U_b(t)=\frac{1}{2}EI\int_0^L\left(\frac{\partial^2\omega(x,t)}{\partial x^2}\right)^2\mathrm{d}x+\frac{1}{2}\rho A\int_0^L\left(\frac{\partial\omega(x,t)}{\partial t}\right)^2\mathrm{d}x \tag{11}$$

In the current case, the problem of dynamic optimization is formulated as follows:

$$\min_{m_ic_ik_ix_i\theta_iC_{pi}R_i}\int_0^{t_f}E_b(t)\,\mathrm{d}t \tag{12}$$

subject to system (10), which corresponds the equality constraints of the dynamic optimization problem.

We equip the beam with a set of absorbers and piezoelectric elements, as shown in Fig. 3. Jacquot [34] treated this system, without harvesting devices, for steady-state vibration optimization. We first apply the Galerkin method to discretize the governing equations and associated boundary conditions using the first m beam mode shapes. Consequently, the displacement $w(x,t)$ at location x along the beam and time t is expressed as

$$w(x,t)=\sum_{h=1}^{m}\varphi_h(x)q_h(t) \tag{13}$$

where $q_h(t)$ and $\varphi_h(x)$ denote, respectively, the hth generalized displacement and mode shape. For a simply supported beam, the normalized mode shapes are given by

$$\varphi_h(x)=\sqrt{\frac{2}{L}}\sin\frac{h\pi x}{L} \tag{14}$$

corresponding to the hth natural frequency ω_h given by

$$\omega_h=\frac{h^2\pi^2}{L^2}\sqrt{\frac{EI}{\rho A}} \tag{15}$$

Substituting Eq. (13) into Eqs. (10) yields

$$\begin{aligned}EI\sum_{h=1}^{m}q_h(t)\varphi_h^{iv}(x)+\rho A\sum_{h=1}^{m}\ddot{q}_h(t)\varphi_h(x)=&-\sum_{i=1}^{n}k_i\Big(\sum_{h=1}^{m}[q_h(t)\varphi_h(x)-z_i]\delta(x-x_i)\Big)\\&-\sum_{i=1}^{n}c_i\Big(\sum_{h=1}^{m}[\dot{q}_h(t)\varphi_h(x)-\dot{z}_i]\delta(x-x_i)\Big)\end{aligned} \tag{16a}$$

$$m_i\ddot{z}_i+c_i\dot{z}_i+k_iz_i-\frac{\theta_i}{C_{pi}}Q_i=k_i\sum_{h=1}^{m}q_h(t)\varphi_h(x_i)+c_i\sum_{h=1}^{m}\dot{q}_h(t)\varphi_h(x_i)\quad \text{for } i=1,2,\ldots,n \tag{16b}$$

$$R_i\dot{Q}_i-\frac{\theta_i}{C_{pi}}\Big(z_i-\sum_{h=1}^{m}q_h(t)\varphi_h(x_i)\Big)+\frac{Q_i}{C_{pi}}=0\quad \text{for } i=1,2,\ldots,n \tag{16c}$$

Multiplying Eqs. (16) by $(1/\rho A)\varphi_r(x)$ and integrating the resulting equation from 0 to L leads to

$$\ddot{q}_r(t)+\omega_r^2q_r(t)=-\sum_{i=1}^{n}k_i\Big(\sum_{h=1}^{m}q_h(t)\varphi_h(x_i)\varphi_r(x_i)-z_i\varphi_r(x_i)\Big)/\rho A-\sum_{i=1}^{n}c_i\Big(\sum_{h=1}^{m}\dot{q}_h(t)\varphi_h(x_i)\varphi_r(x_i)-\dot{z}_i\varphi_r(x_i)\Big)/\rho A \tag{17}$$

The equations of motion, described by Eqs. (16b) and (17), can be put in the following matrix form:

$$\ddot{Y} + C\dot{Y} + KY = F \tag{18}$$

where

$$Y^T = [q_1 \;\; q_2 \;\; \dots \;\; q_m \;\; z_1 \;\; z_2 \;\; \dots \;\; z_n], F^T = \left[0_{1\times m} \;\; \frac{\theta_1}{C_{p1}}Q_1 \;\; \frac{\theta_2}{C_{p2}}Q_2 \;\; \dots \;\; \frac{\theta_n}{C_{pn}}Q_n\right]$$

and the mass, damping, and stiffness matrices are given by

$$C = \begin{bmatrix} \Theta_D & -\dfrac{V}{\rho A} \\ -M_a^{-1}V^T & M_a^{-1}D \end{bmatrix}, K = \begin{bmatrix} \Theta_S & -\dfrac{G}{\rho A} \\ -M_a^{-1}G^T & M_a^{-1}B \end{bmatrix} \tag{19}$$

$$\Theta_D = \frac{1}{\rho A}\sum_{i=1}^{n} c_i\Theta_i, \Theta_i = \begin{bmatrix} \varphi_1^2(x_i) & \varphi_2(x_i)\varphi_1(x_i) & \dots & \varphi_m(x_i)\varphi_1(x_i) \\ \varphi_1(x_i)\varphi_2(x_i) & \varphi_2^2(x_i) & \dots & \varphi_m(x_i)\varphi_2(x_i) \\ \vdots & \vdots & \ddots & \vdots \\ \varphi_1(x_i)\varphi_m(x_i) & \dots & \varphi_{m-1}(x_i)\varphi_m(x_i) & \varphi_m^2(x_i) \end{bmatrix}$$

$$V = \begin{bmatrix} c_1\varphi_1(x_1) & c_2\varphi_1(x_2) & \dots & c_n\varphi_1(x_n) \\ c_1\varphi_2(x_1) & c_2\varphi_2(x_2) & \cdots & c_n\varphi_2(x_n) \\ \vdots & \vdots & \ddots & \vdots \\ c_1\varphi_m(x_1) & c_2\varphi_m(x_2) & \dots & c_n\varphi_m(x_n) \end{bmatrix}, D = \begin{bmatrix} c_1 & 0 & \dots & 0 \\ 0 & c_2 & \ddots & \vdots \\ \vdots & \ddots & \ddots & 0 \\ 0 & \dots & 0 & c_n \end{bmatrix}$$

$$B = \begin{bmatrix} k_1 & 0 & \dots & 0 \\ 0 & k_2 & \ddots & \vdots \\ \vdots & \ddots & \ddots & 0 \\ 0 & \dots & 0 & k_n \end{bmatrix}, \Theta_S = \Omega + \frac{1}{\rho A}\sum_{i=1}^{n} k_i\Theta_i, \Omega = \begin{bmatrix} \omega_1^2 & 0 & \dots & 0 \\ 0 & \omega_2^2 & \ddots & \vdots \\ \vdots & \ddots & \ddots & 0 \\ 0 & \dots & 0 & \omega_m^2 \end{bmatrix}$$

$$G = \begin{bmatrix} k_1\varphi_1(x_1) & k_2\varphi_1(x_2) & \dots & k_n\varphi_1(x_n) \\ k_1\varphi_2(x_1) & k_2\varphi_2(x_2) & \cdots & k_n\varphi_2(x_n) \\ \vdots & \vdots & \ddots & \vdots \\ k_1\varphi_m(x_1) & k_2\varphi_m(x_2) & \dots & k_n\varphi_m(x_n) \end{bmatrix}, M_a = \begin{bmatrix} m_1 & 0 & \dots & 0 \\ 0 & m_2 & \ddots & \vdots \\ \vdots & \ddots & \ddots & 0 \\ 0 & \dots & 0 & m_n \end{bmatrix}$$

and $N = m + n$. We put Eqs. (18) and (16c) in the following first-order form:

$$\begin{bmatrix} \dot{U} \\ \dot{Q} \end{bmatrix} = \begin{bmatrix} A_{11} & A_{12} \\ A_{21} & A_{22} \end{bmatrix}\begin{bmatrix} U \\ Q \end{bmatrix} \tag{20}$$

where

$$U^T = [Y^T \;\; \dot{Y}^T], A_{11} = \begin{bmatrix} 0 & I \\ -K & -C \end{bmatrix}, A_{12} = \begin{bmatrix} 0_{(N+m)\times n} \\ B_{12} \end{bmatrix}, A_{21} = [B_{21} \;\; C_{21} \;\; 0_{n\times N}]$$

$$A_{22} = -\begin{bmatrix} \dfrac{1}{R_1C_{p1}} & 0 & \dots & 0 \\ 0 & \dfrac{1}{R_2C_{p2}} & \ddots & \vdots \\ \vdots & \ddots & \ddots & 0 \\ 0 & \dots & 0 & \dfrac{1}{R_nC_{pn}} \end{bmatrix}, B_{12} = \begin{bmatrix} \dfrac{\theta_1}{m_1C_{p1}} & 0 & \dots & 0 \\ 0 & \dfrac{\theta_2}{m_2C_{p2}} & \ddots & \vdots \\ \vdots & \ddots & \ddots & 0 \\ 0 & \cdots & 0 & \dfrac{\theta_n}{m_nC_{pn}} \end{bmatrix}$$

$$B_{21} = -\begin{bmatrix} \dfrac{\theta_1}{R_1C_{p1}}\varphi_1(x_1) & \dfrac{\theta_1}{R_1C_{p1}}\varphi_2(x_1) & \dots & \dfrac{\theta_1}{R_1C_{p1}}\varphi_m(x_1) \\ \dfrac{\theta_2}{R_2C_{p2}}\varphi_1(x_2) & \ddots & \ddots & \dfrac{\theta_2}{R_2C_{p2}}\varphi_m(x_2) \\ \vdots & \ddots & \ddots & \vdots \\ \dfrac{\theta_n}{R_nC_{pn}}\varphi_1(x_n) & \dfrac{\theta_n}{R_nC_{pn}}\varphi_2(x_n) & \dots & \dfrac{\theta_n}{R_nC_{pn}}\varphi_m(x_n) \end{bmatrix}, C_{21} = \begin{bmatrix} \dfrac{\theta_1}{R_1C_{p1}} & 0 & \dots & 0 \\ 0 & \dfrac{\theta_2}{R_2C_{p2}} & \ddots & \vdots \\ \vdots & \ddots & \ddots & 0 \\ 0 & \dots & 0 & \dfrac{\theta_n}{R_nC_{pn}} \end{bmatrix}$$

In case the beam damping is of the proportional type; that is,

$$\Gamma = \alpha I_{m\times m} + \beta\Omega \tag{21}$$

where α and β are real, the augmented damping matrix simplifies to

$$C = \begin{bmatrix} \Gamma + \Theta_D & -\dfrac{V}{\rho A} \\ -M_a^{-1}V^T & M_a^{-1}D \end{bmatrix} \tag{22}$$

We set the damping coefficients

$$c_i = 2\xi_i\sqrt{m_i k_i} \tag{23}$$

where ξ_i is the damping coefficient of the ith absorber, as equality constraints. For a simply supported beam, $\varphi_h(x)$ is given by Eq. (14) and the dynamic optimization problem simplifies to

$$\min_{m_i c_i k_i x_i \theta_i C_{pi} R_i} \int_0^{t_f} \frac{\rho A}{2}(\dot{q}_h^2(t) + \omega_h^2 q_h^2(t))\,\mathrm{d}t \tag{24}$$

$$\begin{gathered} \text{subject to } \begin{bmatrix} \dot{U} \\ \dot{Q} \end{bmatrix} = \begin{bmatrix} A_{11} & A_{12} \\ A_{21} & A_{22} \end{bmatrix} \begin{bmatrix} U \\ Q \end{bmatrix} \\ c_i - 2\xi_i\sqrt{m_i k_i} = 0 \\ k^L \le k_i \le k^U \\ c^L \le c_i \le c^U \\ m^L \le m_i \le m^U \\ x^L \le x_i \le x^U \\ \theta^L \le \theta_i \le \theta^U \\ C_p^L \le C_{pi} \le C_p^U \\ R^L \le R_i \le R^U \quad \text{for } i = 1,2,\ldots,n \end{gathered} \tag{25}$$

5. Configuration 2

In this case, the piezoelectric elements are embedded between the ground and the absorber masses. The equations of motion are given by

$$EI\frac{\partial^4 w(x,t)}{\partial x^4} + \rho A\frac{\partial^2 w(x,t)}{\partial t^2} = -\sum_{i=1}^{n}\left[k_i(w(x_i,t) - z_i) + c_i\left(\frac{\partial w(x_i,t)}{\partial t} - \dot{z}_i\right)\right]\delta(x - x_i) \tag{26a}$$

$$m_i\ddot{z}_i + c_i\dot{z}_i + k_i z_i - \frac{\theta_i}{C_{pi}}Q_i = k_i w(x_i,t) + c_i\frac{\partial w(x_i,t)}{\partial t} \quad \text{for } i = 1,2,\ldots,n \tag{26b}$$

$$R_i\dot{Q}_i - \frac{\theta_i}{C_{pi}}z_i + \frac{Q_i}{C_{pi}} = 0 \quad \text{for } i = 1,2,\ldots,n \tag{26c}$$

and the problem of dynamic optimization is formulated as follows:

$$\min_{m_i c_i k_i x_i \theta_i C_{pi} R_i} \int_0^{t_f} E_b(t)\,\mathrm{d}t \tag{27}$$

subject to Eq. (26). Similarly, using proportional damping, we find that the dynamics of the augmented structure can be described by

$$\begin{bmatrix} \dot{U} \\ \dot{Q} \end{bmatrix} = \begin{bmatrix} A_{11} & A_{12} \\ A_{21} & A_{22} \end{bmatrix} \begin{bmatrix} U \\ Q \end{bmatrix} \tag{28}$$

where U, A_{11}, A_{12}, and A_{22} remain the same and A_{21} becomes

$$A_{21} = \begin{bmatrix} 0_{n\times m} & C_{21} & 0_{n\times N} \end{bmatrix}$$

Finally, the dynamic optimization problem consists of $N+n$ ordinary-differential equations as linear equality constraints and n nonlinear equality constraints. Fig. 5 shows a flowchart of the proposed algorithm for solving the dynamic optimization problem. During the flow of energy within the structure, the absorbers experience larger vibration amplitudes, and, thus, a system for energy harvesting is integrated to convert the mechanical energy into electrical power. This conversion was largely investigated by studies, such as those by Sodano et al. [1], Onoda et al. [35], Lefeuvre et al. [8]

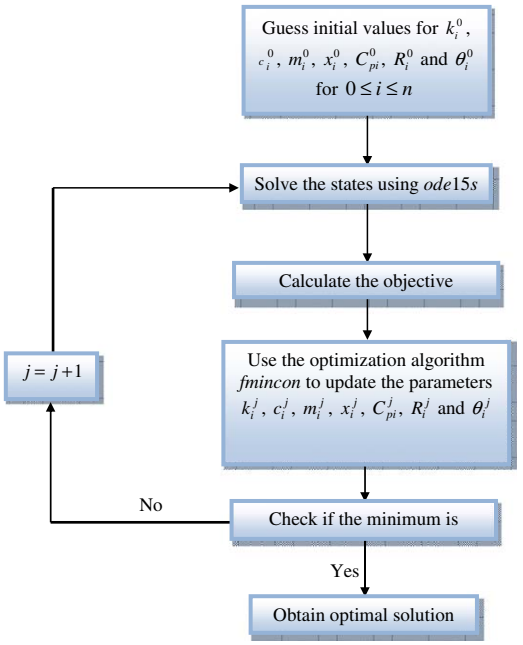

Fig. 5. Flowchart of the dynamic optimization algorithm.

Table 1
Optimized mechanical parameters of the controlled structure with 3, 4 and 5 modes.

Optimized parameters	m_1 (kg)	m_2 (kg)	m_3 (kg)	k_1 (N/m)	k_2 (N/m)	k_3 (N/m)	x_1 (m)	x_2 (m)	x_3 (m)	c_1 (N s/m)	c_2 (N s/m)	c_3 (N s/m)
First configuration												
3 modes	0.0951	0.0902	0.0951	1570.4	1022.4	1572.2	0.4999	0.5002	0.5000	0.2444	0.1921	0.2446
4 modes	0.0951	0.0905	0.0951	1570.4	1022.4	1572.2	0.4676	0.4843	0.4681	0.2444	0.1921	0.2446
5 modes	0.0951	0.0905	0.0951	1570.4	1022.4	1572.2	0.4676	0.4843	0.4681	0.2444	0.1924	0.2446

Table 2
Optimized piezoelectric parameters of the controlled structure with 3, 4 and 5 modes.

Optimized parameters	θ_1 (C/m)	θ_2 (C/m)	θ_3 (C/m)	C_{p1} (μF)	C_{p2} (μF)	C_{p3} (μF)	R_1 (Ω)	R_2 (Ω)	R_3 (Ω)
First configuration									
3 modes	0.01	0.01	0.01	1.00	1.00	1.00	1e+5	1e+5	1e+5
4 modes	0.01	0.01	0.01	1.00	1.00	1.00	1e+5	1e+5	1e+5
5 modes	0.01	0.01	0.01	1.00	1.00	1.00	1e+5	1e+5	1e+5

and Faiz et al. [36]. The addition of absorbers and piezoelectric elements can also be used for the purpose of improving damping of the original structure.

6. Simulations and discussion

We consider a simply supported beam of length $L = 1$ m, density $\rho = 2700\,\mathrm{kg/m^3}$, Young's modulus $E = 7 \times 10^{10}\,\mathrm{N/m^2}$, second moment of area $I = 4.167 \times 10^{-9}\,\mathrm{m^4}$, and cross-section area $A = 5 \times 10^{-4}\,\mathrm{m^2}$. We add three sets of collocated absorbers and piezoelectric elements at locations x_i $(i = 1, 2, 3)$ (see Figs. 3 and 4). We developed a computer code that uses the *fmincon* command in Matlab to determine a local optimized solution. The command *ode*15 *s* numerically integrates the discretized set of ordinary-differential equations subject to upper and lower bounds on the parameters of the absorbers and piezoelectric elements.

We emphasize that the optimized parameters of the absorbers must be insensitive to the number of modes considered in the approximation of the beam dynamics. To prove this, we ran our code for different numbers of modes (3, 4 and 5) and $\xi_1 = \xi_2 = \xi_3 = 1$ percent. The resulting sets of mechanical and electrical parameters are displayed in Tables 1 and 2, respectively. Whereas the electrical parameters are unchanged, we note that the mechanical parameters are not

significantly changed as the number of modes is varied from 3 to 5. Also, Figs. (6–10) display performances of the beam-absorber system for 3 modes (solid—blue), 4 modes (dashed—red), and 5 modes (dotted—black). We note that the time responses of the beam and absorbers are not significantly altered as the number of modes is varied from 3 to 5.

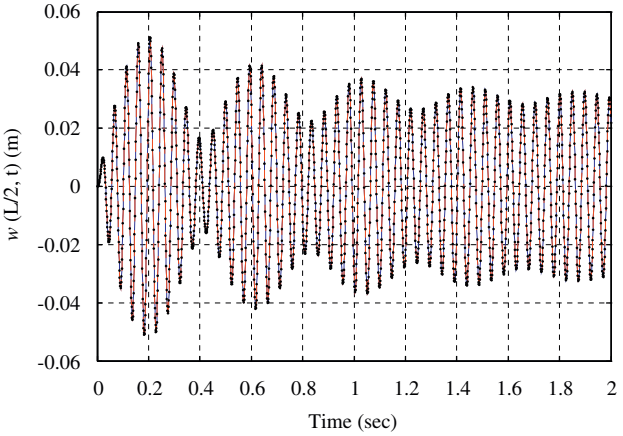

Fig. 6. Uncontrolled displacement of the beam midpoint associated with configuration 1 using 3 modes (solid—blue), 4 modes (dashed—red), and 5 modes (dotted—black). (For interpretation of the references to color in this figure legend, the reader is referred to the webversion of this article.)

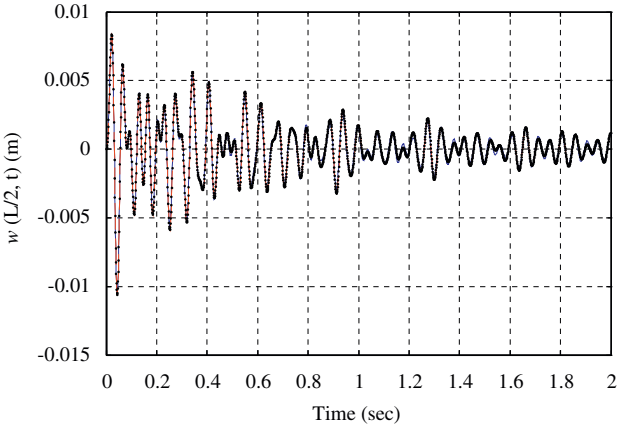

Fig. 7. Controlled displacement of the beam midpoint associated with configuration 1 using 3 modes (solid—blue), 4 modes (dashed—red), and 5 modes (dotted—black). (For interpretation of the references to color in this figure legend, the reader is referred to the webversion of this article.)

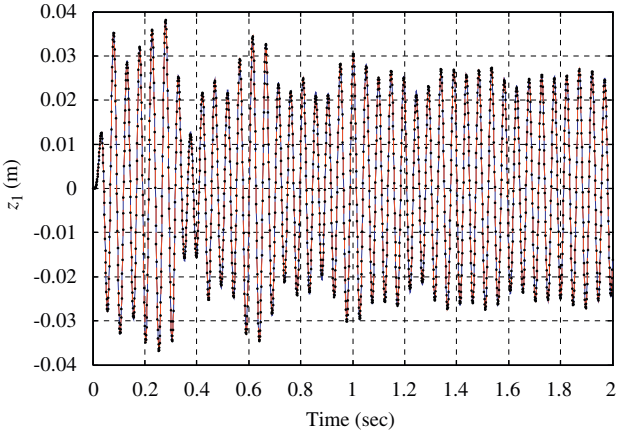

Fig. 8. Displacement of the first absorber associated with configuration 1 using 3 modes (solid—blue), 4 modes (dashed—red), and 5 modes (dotted—black); $\xi_1 = 1\%$. (For interpretation of the references to color in this figure legend, the reader is referred to the webversion of this article.)

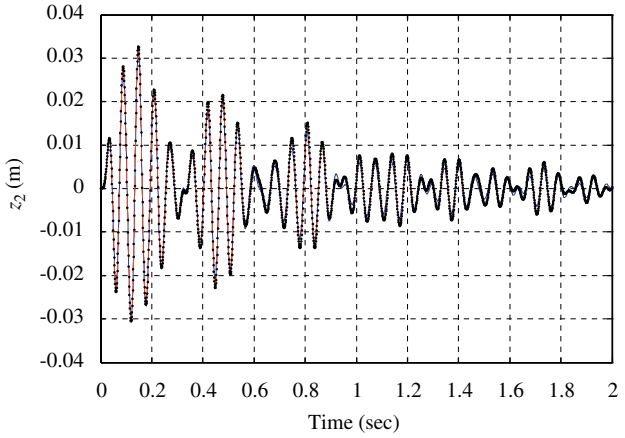

Fig. 9. Displacement of the second absorber associated with configuration 1 using 3 modes (solid—blue), 4 modes (dashed—red), and 5 modes (dotted—black); $\xi_2 = 1\%$. (For interpretation of the references to color in this figure legend, the reader is referred to the webversion of this article.)

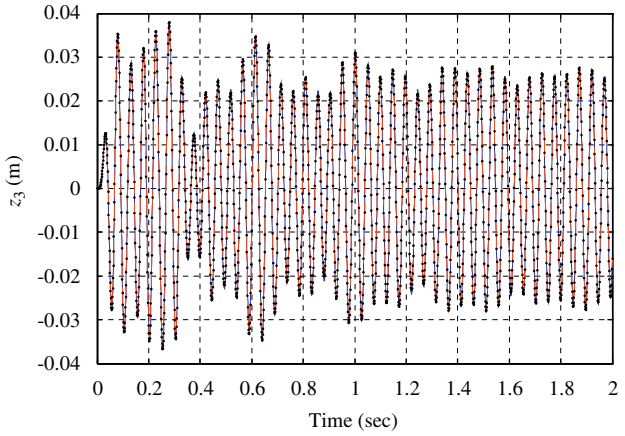

Fig. 10. Displacement of the third absorber associated with configuration 1 using 3 modes (solid—blue), 4 modes (dashed—red), and 5 modes (dotted—black); $\xi_3 = 1\%$. (For interpretation of the references to color in this figure legend, the reader is referred to the webversion of this article.)

Table 3
Optimized mechanical parameters of the controlled structure using 3 modes.

Optimized parameters	m_1 (kg)	m_2 (kg)	m_3 (kg)	k_1 (N/m)	k_2 (N/m)	k_3 (N/m)	x_1 (m)	x_2 (m)	x_3 (m)	c_1 (N s/m)	c_2 (N s/m)	c_3 (N s/m)
First configuration	0.0951	0.0931	0.0951	1570.4	1022.4	1572.2	0.4999	0.4999	0.5000	0.7332	0.5855	0.7337
Second configuration	0.0951	0.095	0.0951	1570.4	1022.4	1572.2	0.5000	0.5001	0.5001	0.7332	0.5914	0.7337

Using a three-mode approximation, we first optimize the total energy of the beam subject to the set of ordinary-differential equations, which describe the proportionally damped dynamics of the beam-absorber-piezo system in the first configuration (see Fig. 3). Then, we optimize the same energy subject to the set of ordinary-differential equations, which describe the proportionally damped beam-absorbers-harvesting system in the second configuration (see Fig. 4). For the damping of the beam-absorber system, we let $\alpha = 2.1664$ and $\beta = 3.4926 \times 10^{-5}$ to produce $\xi_1 = 0.01$, $\xi_2 = 0.012$, and $\xi_3 = 0.0236$ (first three damping ratios of the beam). We also select damping ratios of the absorbers as $\xi_1 = \xi_2 = \xi_3 = 0.03$, given in Eq. (23). To check the viability of the design, we set all initial conditions equal to zero and consider the external harmonic excitations $F_i(t) = 50 \sin 130t$ $(i = 1, 2)$ applied at $x_1 = (1/3)L$ and $x_2 = (2/3)L$ in both configurations.

The resulting optimized parameters of the absorbers are summarized in Table 3 for the both configurations. Table 4 summarizes the resulting electrical parameters. We note that a different set of mechanical and electrical parameters is obtained for each case. We first display the time response of the beam midpoint without absorber-piezo systems in Fig. 11a. With the addition of the passive elements, Figs. 11b–e show the displacement of the beam midpoint and those of the absorbers for the first configuration. We note that the vibration energy is confined in the absorbers and then harvested by

Table 4
Optimized piezoelectric parameters of the controlled structure using 3 modes.

Optimized parameters	θ_1 (C/m)	θ_2 (C/m)	θ_3 (C/m)	C_{p1} (μF)	C_{p2} (μF)	C_{p3} (μF)	R_1 (Ω)	R_2 (Ω)	R_3 (Ω)
First configuration	0.01	0.0075	0.01	1.00	5.00	1.00	1e+5	1e+5	1e+5
Second configuration	0.0075	0.01	0.0075	5.00	1.00	5.00	1e+5	1e+5	1e+5

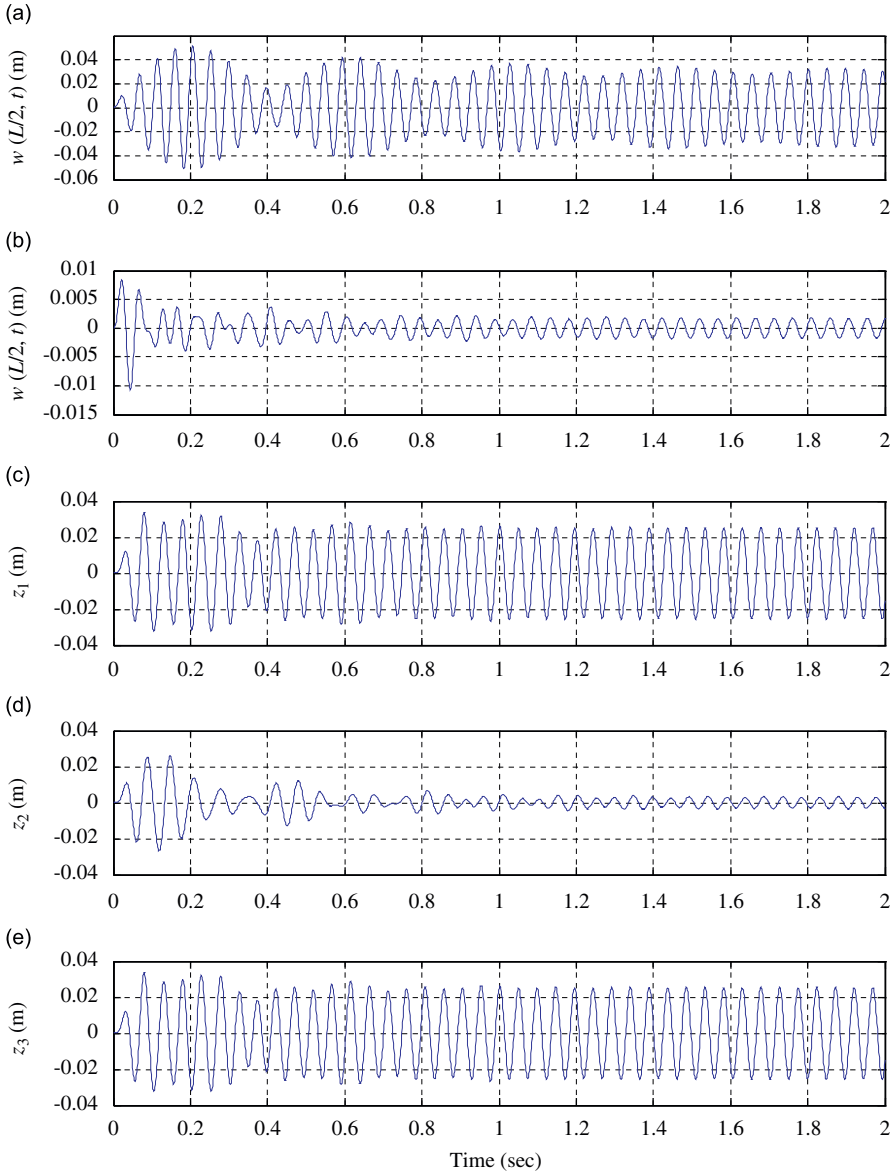

Fig. 11. Displacement of the damped beam midpoint and absorbers associated with configuration 1; (a) uncontrolled beam midpoint; (b) controlled beam midpoint; (c) first absorber; (d) second absorber; (e) third absorber; $\xi_1 = \xi_2 = \xi_3 = 3\%$.

the piezoelectric devices. At time $t = 0.9$ s, the vibration energy of the beam is suppressed (Fig. 11b). Figs. 12a–f show the harvested powers (P_i for $i = 1, 2, 3$) and the piezoelectric voltages (V_i for $i = 1, 2, 3$) for excitation case 2 and configuration 2. We observe that the maximum harvested powers occur between the time period [0 0.8] s.

Table 5 gives the eigenvalues and frequencies of the controlled damped structure associated with the second excitation case and the first configuration. We note that all real parts of the eigenvalues are negative, and thus the altered structure is asymptotically stable. The first three frequencies of the uncontrolled beam are 145.1, 580.3 and 1305.6 rad/s and the first three frequencies of the controlled beam are 180.7, 580.2 and 1308 rad/s. We note that the first frequency of the controlled

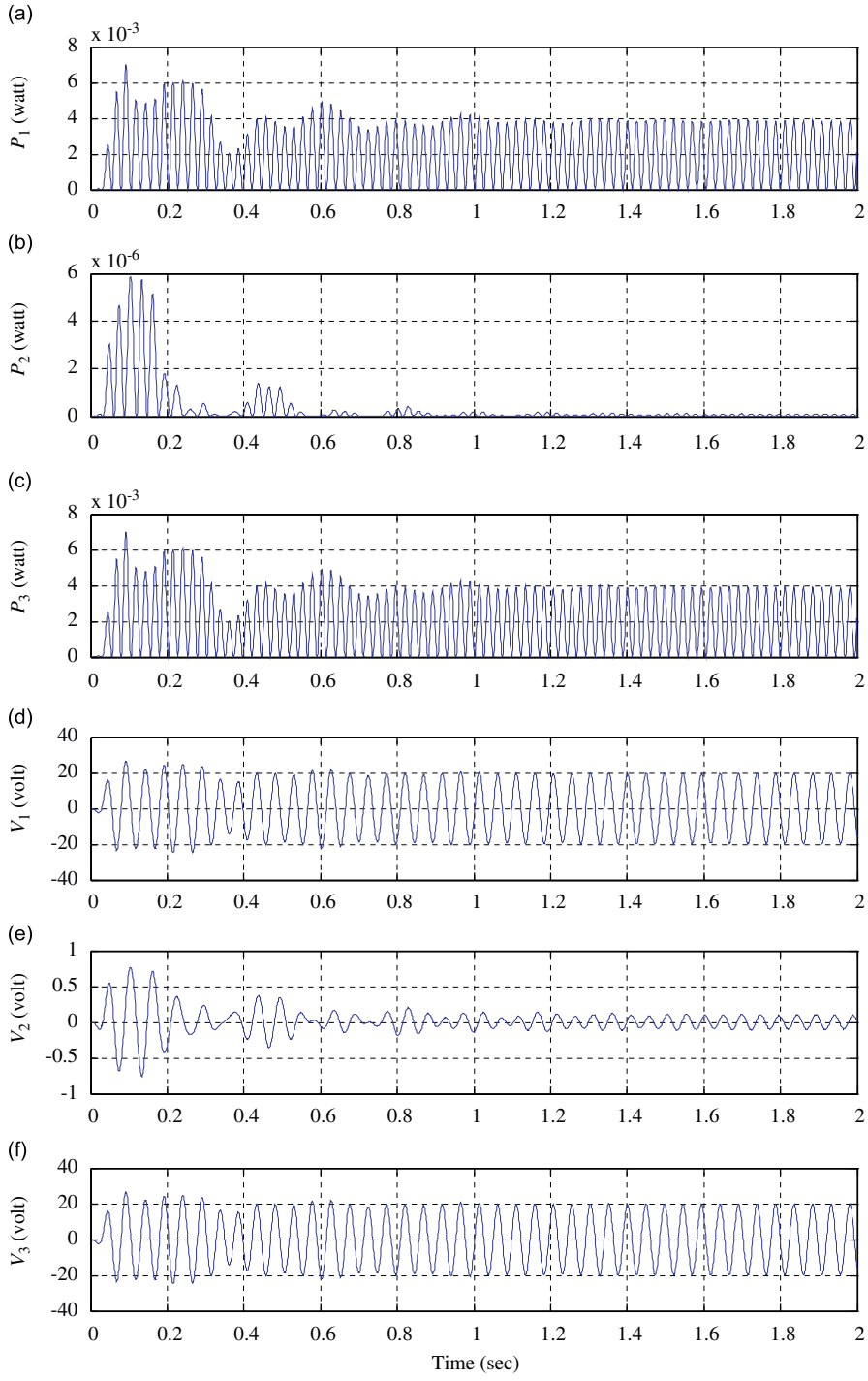

Fig. 12. Harvested powers and piezoelectric voltages of the vibration energy associated with configuration 1: (a) first piezoelectric power, (b) second piezoelectric power, (c) third piezoelectric power, (d) first piezoelectric voltage, (e) second piezoelectric voltage, (f) third piezoelectric voltage.

beam is increased, while the other two frequencies are hardly changed. Before their addition, the frequencies of absorbers are 104.8, 128.5 and 128.58 rad/s. After addition, these frequencies are lowered to 94.5, 114.2 and 128.6 rad/s. This implies that, for simultaneous confinement and harvesting, the beam must be stiffened and the absorbers must be softened to allow the transfer of vibration energy.

In the presence of absorbers and piezoelectric elements, Fig. 13 shows the displacement of the beam midpoint in the both configurations. We note that the second configuration yields faster extraction of vibration energy, which is clearly confined in the absorbers and then harvested.

Table 5
Eigenvalues of the controlled damped structure associated with piezoelectric configuration 1.

Beam		Absorbers			Harvesting system	
Eigenvalues	Frequencies	Eigenvalues	Frequencies	Frequencies before adding	Eigenvalues	Frequencies
$-5.2\pm180.6i$	180.7	$-2.4\pm94.5i$	94.5	104.8	−20	20
$-7\pm580.2i$	580.2	$-3.5\pm114.1i$	114.2	128.5	−94	94
$-32.4\pm1307.6i$	1308	$-4.2\pm128.5i$	128.6	128.58	−94	94

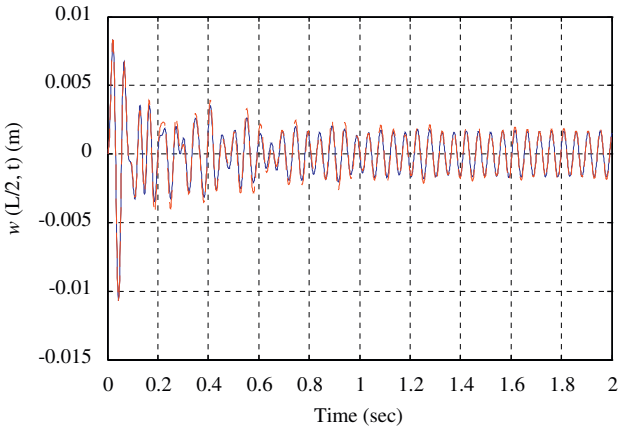

Fig. 13. Controlled displacement of the beam midpoint associated with piezoelectric configuration 1 (dashed—red); piezoelectric configuration 2 (solid—blue). (For interpretation of the references to color in this figure legend, the reader is referred to the webversion of this article.)

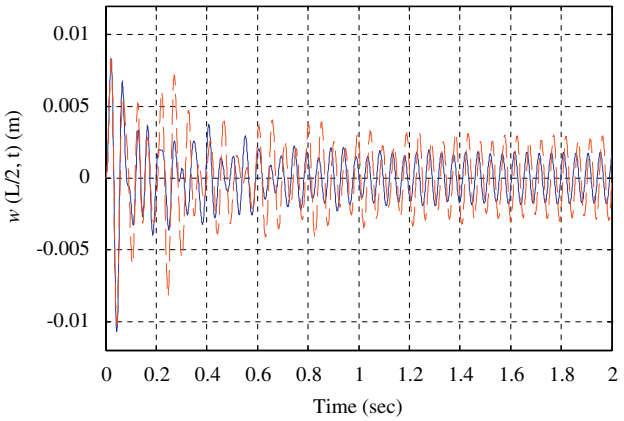

Fig. 14. Controlled displacement of the beam midpoint associated with piezoelectric configuration 1; optimized parameters (solid—blue); perturbed parameters (dashed—red). (For interpretation of the references to color in this figure legend, the reader is referred to the webversion of this article.)

In the presence of passive elements and harvesting systems, Figs. 14 and 15(a, b, c) display the displacements of the beam midpoint and the three absorbers, respectively, associated with the second case of excitation and the first configuration of the piezoelectric elements. Fig. 16 shows the frequency responses of the beam midpoint with and without control. It clearly demonstrates the effects of the absorbers in attenuating the vibrational energy in the sensitive beam. To compare performance of the optimized and nonoptimized structures, we perturb the optimized stiffnesses by 10 percent. We observe that the vibration energy is better confined in the optimized case (solid—blue) as compared to the perturbed case (dashed—red). They are given by $k_1^0 = 1.7274\,\mathrm{kN/m}$, $k_2^0 = 1.1246\,\mathrm{kN/m}$, $k_3^0 = 1.7294\,\mathrm{kN/m}$. We verified that the computer code yielded the same set of optimized parameters, which are listed in Table 3—configuration 1 and Table 4—configuration 1.

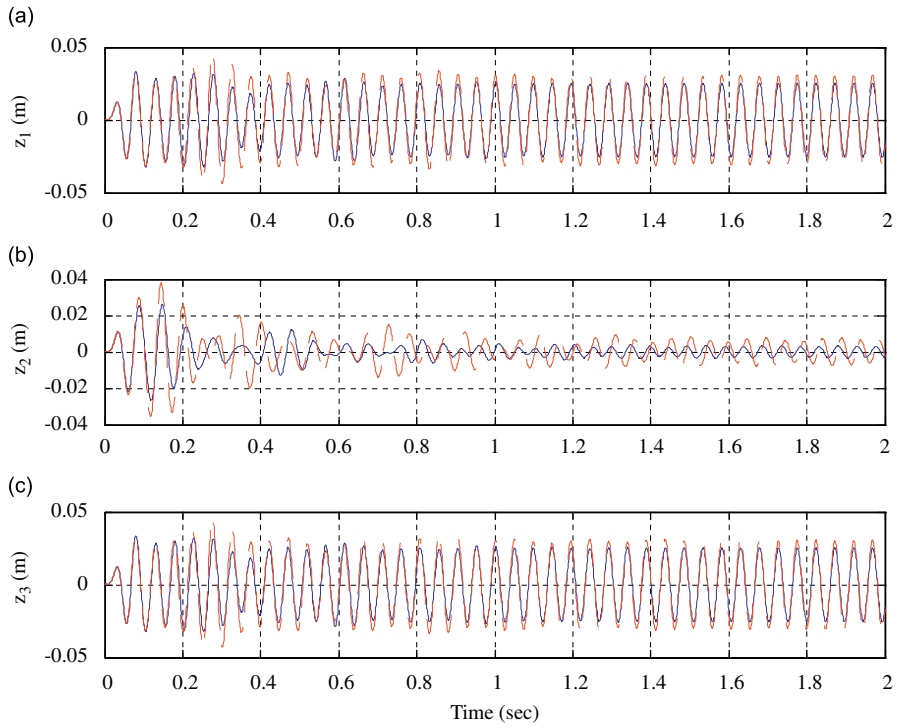

Fig. 15. Displacement of the absorbers associated with piezoelectric configuration 1; optimized parameters (solid—blue); perturbed parameters (dashed—red): (a) first absorber, (b) second absorber, (c) third absorber; $\xi_1 = \xi_2 = \xi_3 = 3\%$. (For interpretation of the references to color in this figure legend, the reader is referred to the webversion of this article.)

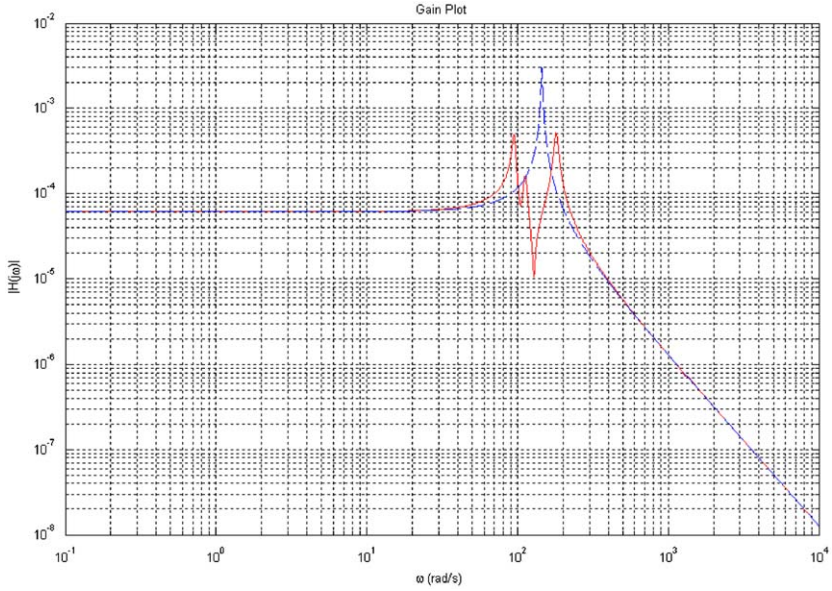

Fig. 16. Frequency responses of the controlled (solid) and uncontrolled (dashed) beam midpoint to a single excitation $u(t)$ at $L/3(H(jw) = w(L/2, jw)/u(jw))$.

7. Conclusions

We proposed a strategy for optimizing the parameters of a set of collocated pairs of absorbers and piezoelectric systems for confining and harvesting the vibration of flexible structures. We formulated the design of these absorbers and harvesting systems as a dynamic optimization problem in which the objective function is the total energy of the unaltered structure. Using the Galerkin procedure, we discretized the dynamics of the structure equipped with the added absorbers

and the piezoelectric systems. We wrote a Matlab code to optimize the locations, masses, stiffnesses, and damping coefficients of the absorbers, and the capacitances, load resistances, and electromechanical coupling coefficients of the piezoelectric elements to minimize the total energy of the original structure. We first supplied a set of initial values for these parameters, and the code updated them while minimizing the total energy in the uncontrolled structure. We simulated the performance of a simply supported beam with external excitations and showed that the vibration energy is confined to the absorbers and then harvested as electric power.

References

[1] H.A. Sodano, G. Park, D.J. Inman, Estimation of electric charge output for piezoelectric energy harvesting, *Strain* 40 (2004) 49–58.
[2] J. Feenstra, J. Granstrom, H.A. Sodano, Energy harvesting through a backpack employing a mechanically amplified piezoelectric stack, *Mechanical Systems and Signal Processing* 22 (2008) 721–734.
[3] S.M. Shahruz, Design of mechanical band-pass filters for energy scavenging: multi-degree-of-freedom models, *Journal of Vibration and Control* 14 (5) (2008) 753–768.
[4] N.G. Stephen, On energy harvesting from ambient vibration, *Journal of Sound and Vibration* 293 (2006) 409–425.
[5] T.H. Ng, W.H. Liao, Sensitivity analysis and energy harvesting for a self-powered piezoelectric sensor, *Journal of Intelligent Material Systems and Structures* 16 (2005) 785–797.
[6] P.J. Cornwell, P.J. Goethal, J. Kowko, M. Damianakis, Enhancing power harvesting using a tuned auxiliary structure, *Journal of Intelligent Material Systems and Structures* 16 (2005) 825–834.
[7] H.S. Yoon, G. Washington, A. Danak, Modeling, optimization and design of efficient initially curved piezoceramic unimorphs for energy harvesting applications, *Journal of Intelligent Material Systems and Structures* 16 (2005) 877–888.
[8] E. Lefeuvre, A. Badel, C. Richard, L. Petit, D. Guyomar, A comparison between several vibration-powered piezoelectric generators for standalone systems, *Sensors and Actuators A* 126 (2006) 405–416.
[9] J.Q. Liu, H.B. Fang, Z.Y. Xu, X.H. Mao, X.C. Shen, D. Chen, H. Liao, B.C. Cai, A MEMS-based piezoelectric power generator array for vibration energy harvesting, *Microelectronics Journal* 39 (2008) 802–806.
[10] S.P. Beeby, R.N. Torah, M.J. Tudor, P. Glynne-Jones, T. O'Donnell, C.R. Saha, S. Roy, A micro electromagnetic generator for vibration energy harvesting, *Journal of Micromechanics and Microengineering* 17 (2007) 1257–1265.
[11] M.L. Swallow, J.K. Luo, E. Siores, I. Patel, D. Dodds, A piezoelectric fibre composite based energy harvesting device for potential wearable applications, *Smart Materials and Structures* 17 (2008) 1257–1265.
[12] I. Sari, T. Balkan, H. Kulah, An electromagnetic micro power generator for wideband environmental vibrations, *Sensors and Actuators A* 145–146 (2008) 405–413.
[13] H.A. Sodano, J.S. Bae, D.J. Inman, W.K. Belvin, Improved concept and model of eddy current damper, *Journal of Vibration and Acoustics* 128 (2006) 294–302.
[14] H.A. Sodano, J. Lloyd, J.D. Inman, An experimental comparison between several active composite actuators for power generation, *Smart Materials and Structures* 15 (2006) 1211–1216.
[15] C.B. Williams, R.B. Yates, Analysis of a micro-electric generator for microsystems, *Sensors and Actuators A* 52 (1996) 8–11.
[16] L. Mateu, F. Moll, Appropriate charge control of the storage capacitor in a piezoelectric energy harvesting device for discontinuous load operation, *Sensors and Actuators A* 132 (2006) 302–310.
[17] H.A. Sodano, D.J. Inman, G. Park, Comparison of piezoelectric energy harvesting devices for recharging batteries, *Journal of Intelligent Material Systems and Structures* 16 (2005) 799–807.
[18] G.A. Lesieutre, G.K. Ottman, H.F. Hofmann, Damping as a result of piezoelectric energy harvesting, *Journal of Sound and Vibration* 269 (2004) 991–1001.
[19] H.A. Sodano, D.J. Inman, A review of power harvesting from vibration using piezoelectric materials, *The Shock and Vibration Digest* 36 (3) (2004) 197–205.
[20] Y.B. Jeon, R. Sood, J.H. Jeong, S.G. Kim, MEMS power generator with transverse mode thin film piezoelectric, *Sensors and Actuators A* 122 (2005) 16–22.
[21] G.A. Lesieutre, H.F. Hofmann, G.K. Ottman, Electric power generation from piezoelectric materials, in: *Proceedings of the 13th International Conference on Adaptive Structures and Technologies*, Potsdam/Berlin, Germany, October 7–9, 2002.
[22] T.Y. Wu, K.W. Wang, Periodic isolator design enhancement via vibration confinement through eigenvector assignment and piezoelectric circuitry, *Journal of Vibration and Control* 13 (7) (2007) 989–1006.
[23] H.S. Yoon, Active vibration confinement of flexible structures using piezoceramic patch actuators, *Journal of Intelligent Material Systems and Structures* 19 (2) (2008) 145–155.
[24] A.S. Yigit, S. Choura, Vibration confinement in flexible structures via alteration of mode shapes using feedback, *Journal of Sound and Vibration* 179 (1995) 553–567.
[25] S. Choura, A.S. Yigit, Vibration confinement in flexible structures by distributed feedback, *Computers & Structures* 54 (3) (1995) 531–540.
[26] S. Choura, A.S. Yigit, Confinement and suppression of structural vibrations, *ASME Journal of Vibration and Acoustics* 123 (2001) 496–501.
[27] M. Ouled Chtiba, S. Choura, S. El-Borgi, A.H. Nayfeh, Hybrid control of seismically excited structures by vibration confinement, in: *The Proceedings of the 13th World Conference on Earthquake Engineering*, Vancouver, BC, Canada, August 2004, n.1860.
[28] M. Ouled Chtiba, S. Choura, S. El-Borgi, A.H. Nayfeh, Passive control of flexible structures by confinement of vibrations, *Shock and Vibration* 14 (5) (2007) 321–337.
[29] M. Ouled Chtiba, S. Choura, A.H. Nayfeh, S. El-Borgi, Confinement of vibrations in flexible structures using supplementary absorbers: dynamic optimization, *Journal of Vibration and Control*, 2009, in press.
[30] P. Tanartkit, L.T. Biegler, A nested simultaneous approach for dynamic optimization problems—I, *Computers and Chemical Engineering* 20 (1996) 735–741.
[31] A.M. Cervantes, L.T. Biegler, A stable elemental decomposition for dynamic process optimization, *Journal of Computational and Applied Mathematics* 120 (2000) 41–57.
[32] M.J. Richard, F. Dufour, S. Tarasiewicz, Commande des Robots Manipulateurs par la Programmation Dynamique, *Mechanical Machine Theory* 28 (3) (1993) 301–316.
[33] L.O. Santos, L.T. Biegler, A tool to analyze robust stability for model predictive controllers, *Journal of Process Control* 9 (1999) 233–246.
[34] R.G. Jacquot, Optimal dynamic vibration absorbers for general beam systems, *Journal of Sound and Vibration* 60 (4) (1978) 535–542.
[35] J. Onoda, K. Makihara, K. Minesugi, Energy-recycling semi-active method for vibration suppression with piezoelectric transducers, *AIAA Journal* 41 (4) (2003) 711–719.
[36] A. Faiz, D. Guyomar, L. Petit, C. Buttay, Wave transmission reduction by a piezoelectric semi-passive technique, *Sensors and Actuators A* 128 (2006) 230–237.